Design of Attitude and Heading Reference System Based on MEMS Sensor

Zhiping Liu[1], Lili Wu[2]

1.College of Computer Science and Engineering, Xian Technological University, Xian 710032
E-mail: leopard@xatu.edu.cn

2. College of Computer Science and Engineering, Xian Technological University, Xian 710032
E-mail: wudi1987@163.com

Abstract: This paper presents a design scheme of attitude and heading reference system (AHRS) which consists of low cost MEMS sensors, magnetometers and related data fusion algorithms, based on the chosen sensors and algorithms, the simulation is performed to assess the structure of algorithms, computational burden and convergence from the engineering view of point. Finally, the conclusion was given and related recommendations were proposed.

Key Words: MEMS, Convergence, Data fusion, Low cost

1 INTRODUCTION

With the development of technological breakthrough in the field of micro-electro-mechanical-systems (MEMS), much more low cost MEMS sensors have present undeniable interest for use in many fields, such as motor, robots, medical equipments and military [1]. Various unmanned vehicles need to know their own attitude to be regulated, especially for the unmanned aerial vehicles (UAV) and autonomous underwater vehicles (AUV), the navigation and guidance system has to be equipped on-board. When cost, volume and weight become important constraint factors, the traditional accurate inertial navigation systems have to be substituted by low cost dead reckon system, such as AHRS, especially low cost AHRS. In 2006, Honeywell International has made an integrated guidance, navigation and control flight management unit based on MEMS sensors, it's housed in a small, light weight and low power package and was designed to accommodate the demands of gun-hardened projectiles and missiles [2].

In the previous decades, vertical gyros have been the main attitude sensors for planes, ships and other vehicles, even in some cases, in order to achieve satisfactory precision during several hours, high performance dynamically tuned gyros and accelerometers were blended into the attitude determination system.

Although the AHRS is relatively simple in implementation and low cost compared with accurate inertial navigation systems, the design of hardware architecture and software architecture is still an interesting and challenging work. So in this paper, based on the MEMS sensors we can approach in domestic market, we present the architecture of AHRS, mainly consists of choice of sensors and detailed consideration of data fusion algorithms, simulation of algorithms and assessment, recommendation. This paper is organized as follows. In section 2, the detailed architecture of hardware and software were proposed, the data fusion algorithm was presented in the section 3, the related simulation and result analysis was performed in section 4, finally, the conclusion was drawn and recommendation was given.

2 SCHME OF AHRS

The AHRS was proposed in this paper mainly consists of hard ware and software from the systematic architecture point of view, the hardware include MEMS gyros, MEMS accelerometers, temperature sensor, magnetometers, chips, signal processing circuit, related interfaces, power and mechanical package, correspondingly the software include algorithms of sensor calibration, algorithms of various error compensation, algorithms of navigation computation and data fusion, it should be noted that fault diagnosis scheme is usually incorporated into the software architecture.

Output signals are hybrid analog and digital. A separate magnetometer outputs the Earth magnetic field measurements for magnetic heading determination. The gyro and accelerometer signals are coupled to high speed digital electronics to be used for attitude calculations.

A Selection of sensors

The consideration of choosing sensors mainly focus on it's availability in domestic market, so the MEMS gyros and MEMS accelerometers made by Xi'an China-star M&C limited were selected firstly, magnetometers is chosen also from China-star, main specifications of MEMS gyros, accelerometers and magnetometers can be seen from reference [4], in addition to these sensors, in order to extend the application scope of AHRS, we choose barometer as the auxiliary sensor to estimate the height and air pressure, the specifications of chosen barometer can be found in reference [6].

B System architecture

The systematic architecture of the AHRS incorporates features to meet mechanical, electrical and electronic demands. The proposed AHRS consists of inertial and air pressure sensors, signal conditioning and conversion, digital computation and communication.

This work is supported by Education Reform Program of Xian Technological University under Grant 10JGZ08

The hardware design should consider harsh environment, such as harsh vibration, temperature and electromagnetic variations. The circuit cards are designed with higher than ordinary vibration resonant frequency, this can minimizes the transmission of vibration to the circuit cards, reducing the forces induced from external vibrations, and furthermore it improves the reliability of the processing electronics. The inertial sensors are usually mounted with vibration isolators and attenuator, which not only reduce the computational burden effectively. It also greatly reduces thermal effects from rapidly changing temperatures of ambient air and elements of circuits.

Following is the hardware architecture.

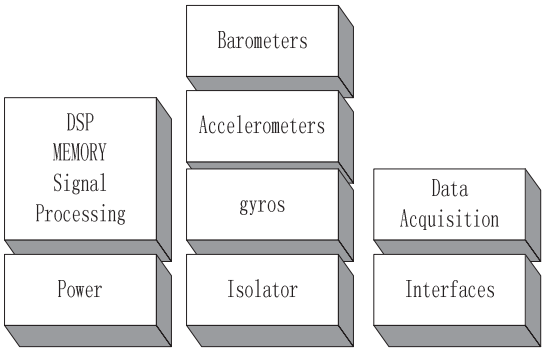

Figure 1 Hardware architecture

Now we discuss the software architecture.

The software runs a deterministic sequence of tasks, each started at a fixed point in time. The tasks are initiated from interrupts generated from a real time clock. The real time clock is maintained from a precision oscillator. The software operates with multiple update rates for the various tasks. Sensor data acquisition is performed at the highest update rate, with the Kalman Filter updates performed at the slowest rate. Air-data and inertial outputs are computed and transmitted at an intermediate update rate. The software has an initial power on mode and then transitions into one of two modes for the remaining time. The software transitions into normal operation mode when installed in a production aircraft. The software has a separate factory mode that is used for calibration, diagnostics, reprogramming and special flight test recording, requiring hardware and software commands in the power-on mode. This factory mode is locked out for normal aircraft installation.

The software reads the sensors, processes the sensor data, and communicates the data to the aircraft on a digital serial bus. The software also performs built in test (BIT) of the different electronic components. BIT includes testing of the sensors, memory and communication circuits. BIT checks input values from the sensors, computed output data and the intermediate computations to ensure they are within their expected ranges. Any detected faults are stored and used later for diagnostic purposes. The software is written in a modular fashion, which allows for code reuse and a greater ease in integrating new functionality. Figure 3 shows the AD-AHRS algorithm overview depicting the data flow from hardware sensors, ARINC-429 inputs and calibration parameters through the top-level modules to ARINC-429 outputs. This modular design allows the system to respond to component and subsystem failures in a robust and graceful fashion. Following is a list of major modules and their functionality:

1).Inertial Sensor Error Compensation module uses calibration data to compensate inertial sensor errors, these errors include random drift, scale errors and environmental induced errors, especially the variation of temperature induced error.

2).Attitude Determination module uses the initial coarse-alignment and body angular rates from the gyros to resolve the attitude and attitude rate. Attitude is propagated in quaternion form to eliminate singularity issues.

3).Data fusion module contains the basic equations that combine the data from the gyro, accelerometer, magnetometer and barometer to give an estimation of attitude and height of the vehicle.

4). Magnetic Heading Determination module determines the magnetic heading. It blends magnetic heading with gyro-bases heading rate to smooth heading angle of high-frequency magnetometer noise and interference, giving so-called gyro-magnetic heading. It uses the magnetic calibration and survey parameters to compensate for in-aircraft magnetic hard and soft iron effects.

5).Altitude calculation module combines air-data barometric altitude and altitude rate with accelerometer data to provide a more responsive barometric altitude and altitude rate. This is the so-called barometer-inertial altitude and altitude rate.

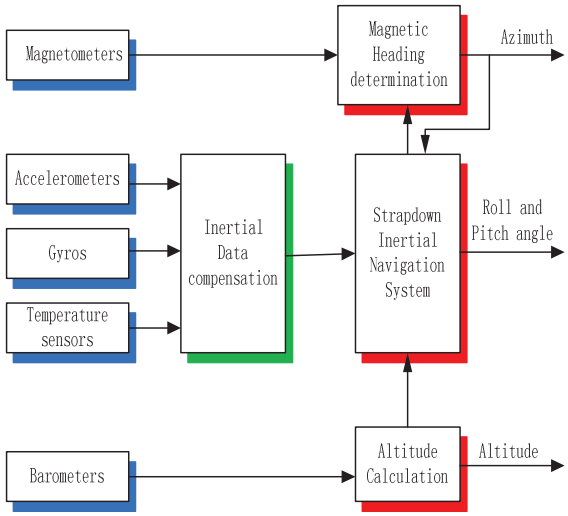

Figure.2 Software architecture

It should be noted that the data fusion modules are distributed in the magnetic heading determination, strapdown inertial navigation system and altitude calculation modules.

In the fig.2, there is a SINS module, its block diagram is depicted as follow in the figure .3, where the ω_{ib}^{b} is the angular rate of body with respect to the inertial frame projected in the body frame, ω_{iL}^{L} is the angular rate of navigation frame with respect to the inertial frame projected

in the navigation frame, R_b^L is the attitude transformation matrix, which transfer the vectors from the vehicle body frame to the navigation frame.

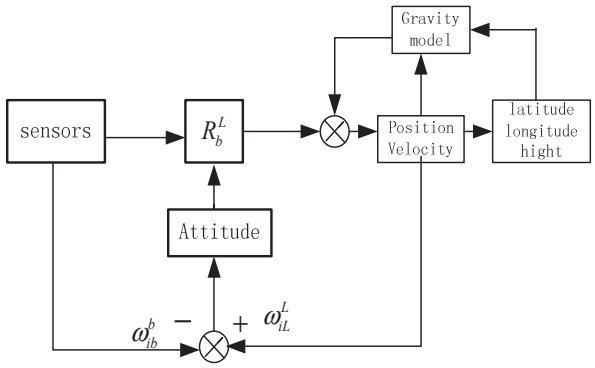

Figure .3 SINS block diagram

In the next section, we will give related algorithms in the software architecture.

3 ALGORITHMS DESCRIPTION

Herein we give the models of the sensors mentioned above in the section 2 and all the algorithms used in this paper.

Firstly, the bias of the MEMS gyros and MEMS accelerometers are modeled as first order Gauss-Markov process, detailed formulas given below.

$$\begin{bmatrix}\dot{b}_x\\ \dot{b}_y\\ \dot{b}_z\end{bmatrix}=-diag(\frac{1}{\tau_{bx}},\frac{1}{\tau_{by}},\frac{1}{\tau_{bz}})\begin{bmatrix}b_x\\ b_y\\ b_z\end{bmatrix}+\begin{bmatrix}w_{bx}\\ w_{by}\\ w_{bz}\end{bmatrix} \tag{1}$$

$$\begin{bmatrix}\dot{d}_x\\ \dot{d}_y\\ \dot{d}_z\end{bmatrix}=-diag(\frac{1}{\tau_{dx}},\frac{1}{\tau_{dy}},\frac{1}{\tau_{dz}})\begin{bmatrix}d_x\\ d_y\\ d_z\end{bmatrix}+\begin{bmatrix}w_{dx}\\ w_{dy}\\ w_{dz}\end{bmatrix} \tag{2}$$

Where the b_i denotes the bias of the MEMS gyros and d_i means the bias of the MEMS accelerometers, τ_{bi} denotes the time constant of Gauss-Markov process of gyro bias and the τ_{di} means the time constant of Gauss-Markov process of accelerometers, w_{bi} and w_{di} are zero mean, Guassian noise.

The calibration models used for gyros and accelerometers are omitted here for the reason of brief.

The height measurement model from the barometer is depicted as follows.

$$\begin{aligned}&H=44330.769\times[1-(\frac{p}{101325})^{0.19026}]\quad H\le 11km\\ &h=\frac{6356766H}{6356766-H}\end{aligned} \tag{3}$$

Where p is the measured pressure, the unit is bar, the unit of height h is m.

The magnetic measurement model from the magnetometers is described as follows [4].

$$\begin{aligned}&\psi=-\arctan[\frac{h_y^h}{h_x^h}]\\ &h^h=(R_\vartheta)^T(R_\gamma)^T h^b\end{aligned} \tag{4}$$

Where ϑ denotes the pitch angle of the vehicle, γ is roll angle of the vehicle, R_ϑ, R_γ is the transformation matrix within the attitude transformation.

The principle of magnetic vector from magnetometer is depicted in the figure.4. Where h^b is the magnetic vector measured in the vehicle frame, h^h is the magnetic vector measured in the navigation frame.

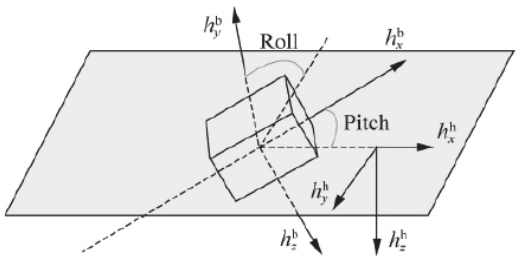

Figure.4 Diagram of magnetic vector transformation

Now we give the complete design of data fusion system. Firstly, indirect filtering algorithm is chosen as data fusion algorithm, the superficial reason is that it could not result in the collapse of the whole estimation system; the deep reason is that this algorithm can be simplified according to the detailed constraints. The states are chosen in the data fusion system are parameter biases, which mean the differences between the measured vectors and their ideal values. The process noise and measurement noise are all chosen as zero-mean Guassian noise.

Detailed formulations of SINS are depicted following, superscript L means the local level frame.

Now we give the complete design of data fusion system. Firstly, indirect filtering algorithm is chosen as data fusion algorithm, the superficial reason is that it could not result in the collapse of the whole estimation system; the deep reason is that this algorithm can be simplified according to the detailed constraints. The states are chosen in the data fusion system are parameter biases, which mean the differences between the measured vectors and their ideal values. The process noise and measurement noise are all chosen as zero-mean Guassian noise.

Detailed formulations of SINS are depicted following, superscript L means the local level frame.

$$\dot{X}^L = \begin{bmatrix} D^{-1}V^L \\ R_b^L f^b - (2\Omega_{ie}^L + \Omega_{eL}^L)V^L + g^L \\ R_B^L \Omega_{iB}^B - \Omega_{iL}^L R_B^L \end{bmatrix} \tag{5}$$

$$X^L = (r^L, V^L, R_B^L)^T \quad r^L = (\varphi, \lambda, h)^T$$

Where φ is the latitude, λ is the longitude, h is the height above the sea level, R_B^L is the attitude transformation matrix, meanings of other symbols can be found in the reference [5].

In the data fusion system, the detailed bias equations used in the SINS are given below.

The position bias equation is depicted as (6).

$$\delta\dot{r}^L = \begin{bmatrix} 0 & 0 & \frac{-\dot{\varphi}}{R_M+h} \\ \dot{\lambda}\tan\varphi & 0 & \frac{-\dot{\lambda}}{R_N+h} \\ 0 & 0 & 0 \end{bmatrix} \delta r^L + \begin{bmatrix} 0 & \frac{1}{(R_M+h)} & 0 \\ \frac{1}{(R_N+h)\cos\varphi} & 0 & 0 \\ 0 & 0 & 1 \end{bmatrix} \delta V^L \tag{6}$$

The bias of velocity equation is described in the (7).

$$\delta\dot{V}^L = \begin{bmatrix} \delta\dot{V}_e \\ \delta\dot{V}_n \\ \delta\dot{V}_u \end{bmatrix} = \begin{bmatrix} 2\omega_e(V_u\sin\varphi + V_n\cos\varphi) + V_n\dot{\lambda}\sec\varphi & 0 & 0 \\ -2\omega_e V_e\cos\varphi - V_e\dot{\lambda}\sec\varphi & 0 & 0 \\ -2\omega_e V_e\sin\varphi & 0 & \frac{2g}{(R_M+h)} \end{bmatrix} \begin{bmatrix} \delta\varphi \\ \delta\lambda \\ \delta h \end{bmatrix}$$

$$+ \begin{bmatrix} \frac{(R_M+h)\dot{\varphi}tg\varphi - \dot{h}}{R_N+h} & (2\omega_e+\dot{\lambda})\sin\varphi & -(2\omega_e+\dot{\lambda})\cos\varphi \\ -(2\omega_e+\dot{\lambda})\sin\varphi & \frac{-\dot{h}}{(R_M+h)} & -\frac{V_n}{R_M+h} \\ (2\omega_e+\dot{\lambda})\cos\varphi & \frac{2V_n}{R_M+h} & 0 \end{bmatrix} \begin{bmatrix} \delta V_e \\ \delta V_n \\ \delta V_u \end{bmatrix} \tag{7}$$

$$+ \begin{bmatrix} 0 & f_u & -f_n \\ -f_u & 0 & f_e \\ f_n & -f_e & 0 \end{bmatrix} \begin{bmatrix} \phi_e \\ \phi_n \\ \phi_u \end{bmatrix} + R_b^L \delta f^b + \delta g^L$$

The attitude bias equation is described in the equation (8). In the calculation of the velocity bias and attitude bias, the needed height is send from the barometer, because the height from the SINS divergences with time.

The azimuth angle is given through the fusion of SINS and magnetometers. Magnetometers could support relative accurate azimuth angle within a long duration, but SINS only give precise azimuth within short duration. From equation (4), we can find that the determination of the azimuth angle still need the accurate pitch angle and roll angle, these two angles are all calculated in the SINS.

It should be noted that the mean of all the symbols in the equation (6), equation (7) and equation (8) can be found in reference [7], for the reason of brief, they are omitted herein.

$$\dot{\phi} = \begin{bmatrix} 0 & (\omega_e\sin\varphi + \frac{V_e tg\varphi}{R_N+h}) & -(\omega_e\cos\varphi + \frac{V_e}{R_N+h}) \\ -(\omega_e\sin\varphi + \frac{V_e tg\varphi}{R_N+h}) & 0 & -\frac{V_n}{R_M+h} \\ (\omega_e\cos\varphi + \frac{V_e}{R_N+h}) & \frac{V_n}{R_M+h} & 0 \end{bmatrix} \phi$$

$$+ \begin{bmatrix} 0 & 0 & -\frac{V_n}{(R_M+h)^2} \\ \omega_e\sin\varphi & 0 & \frac{V_e}{(R_N+h)^2} \\ -(\omega_e\cos\varphi + \frac{V_e}{(R_N+h)\cos^2\varphi}) & 0 & \frac{V_e tg\varphi}{(R_N+h)^2} \end{bmatrix} \begin{bmatrix} \delta\varphi \\ \delta\lambda \\ \delta h \end{bmatrix}$$

$$+ R_b^L \delta\omega_{ib}^b + \begin{bmatrix} 0 & \frac{1}{R_M+h} & 0 \\ \frac{-1}{R_N+h} & 0 & 0 \\ \frac{-tg\varphi}{R_N+h} & 0 & 0 \end{bmatrix} \begin{bmatrix} \delta V_e \\ \delta V_n \\ \delta V_u \end{bmatrix} \tag{8}$$

In the next section, we will give our simulation scheme to emulate the feasibility of the proposed software and assess the property to which the proposed scheme could attain.

4 SIMULATIONS AND ANALYSIS

Theoretically speaking, the simulations of the proposed in this paper should consist of three phases, the first phase is the mathematical simulation; the second simulation is the semi-physical simulation and the third one is the whole physical simulation. Furthermore the van test and flight test are also needed in the practical engineering.

Herein we give the scheme of the first simulation, the simulation module was constructed using MATLAB/SIMULINK, and the diagram of simulation is given below.

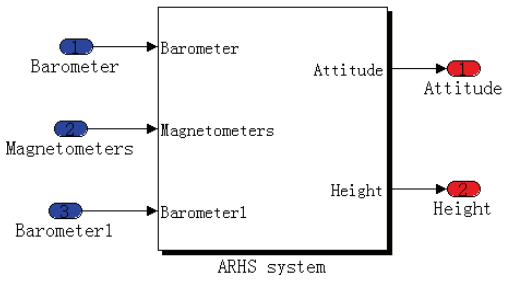

Figure.5 Simulation scheme

As described above, needed data are all from the chosen sensors, when we perform the simulation, the barometer support the height data, the inertial sensors support the angular rates and linear acceleration, the magnetometers

support the magnetic vectors in the vehicle body frame. In the first phase, we collect related data from the laboratory.

The magnetometers we used in the laboratory is the HMR2300, which is the product of the Honeywell corporation. The barometer we used is the product of Taihang Instrument corporation in China.

One of Our objectives in this period is to verify whether the height from the barometer and azimuth from the magnetometers could improve the accuracy of the SINS. Another objective is to verify the feasibility of improving the accuracy in the dynamic environment, which means that the ARHS system is not located in the laboratory, the vehicle has predefined trajectory on the ground, and then in the air.

Now we give the laboratory measurement result and simulation results.

The attitude and height of vehicle from the pure SINS is depicted in the figure.6.and figure.7. When the SINS was Aided by magnetometers and barometers, output of the ARHS is given in the figure .8.

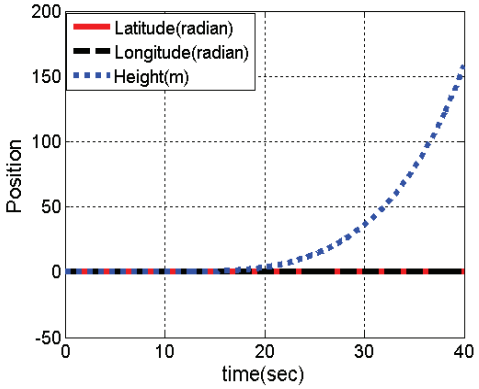

Figure.6 Position from Pure SINS

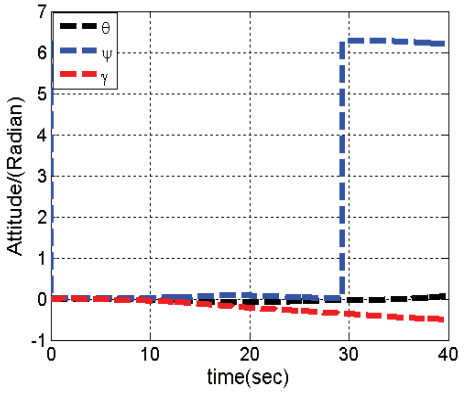

Figure .7 Attitudes from pure SINS

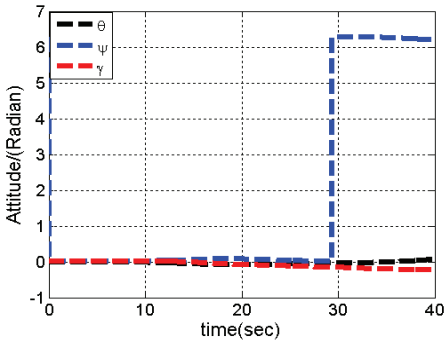

Figure .8 Attitudes from AHRS

From the figure.9, we can see that the accuracy of attitude from ARHS is better than that of pure SINS, and this is basis on which we expand our research work.

5 CONCLUSIONS

In this paper, we present a design scheme of attitude and heading reference system based on low cost MEMS inertial sensors, barometer and magnetometers firstly, then we give detailed algorithms associated with the data fusion and simulation scheme, finally we give the simulation results mainly in the laboratory. Through the mathematical simulation, results validate our proposed design scheme. In the future, challenges we will encounter will be the optimization of algorithms and realization of the practical product.

REFERENCES

[1] J. Wendel, O. Mester, and C. Schlaile, "An integrated GPS/MEMS-IMU navigation system for an autonomous helicopter,"Journal Aerospace Science and Technology, vol. 10, pp. 527–533, May 2006.

[2] T.M. Buck, J.Wilmot, and M.J. Cook, " A high G mems based deeply integrated INS/GPS guidance, navigation and control flight management unit," Proc. IEEE symposium on Position, Location and Navigation, 2006, pp.772-794.

[3] Pressure transmitter, Inertial Navigational Sensor Catelog, 2010 Edition, Chinastar M&C Limited, Xi'an, P.R.China.

[4] Y. Wu, T. Miao and J. Liang, "In-Suit Error Calibration of Three Axis Magnetometer for Unmanned Aerial Vehicle," Acta Aeronautica et Astronautica Sinica, Vol.32, No.2, pp. 330-336, 2011.

[5] D.H. Titterton and J.L. Westone, Strapdown Inertial Navigation Technology, London: Peter Peregrinus, 1997.

[6] Z. Hao and S. Huang, "Development of High Precision Barometric Altimeter,"Journal of Nanjing University of Aeronauotics and Astronautics, Vol.41, No.1,2009, pp.134-138.

[7] Z. Liu and F. Yu, "Observability Analysis and Simulation of Integrated Navigation System During Maneuver," Proceedings of 2011 Chinese Control Conference, July, 2011,pp.3769-3782.

[8] R.M. Rogers, Applied Mathematics in Integrated Navigation System, AIAA Education Series, 2003.

[9] A. Jamshaid and J. Fang, "Realization of Autonomous Integrated Suit of Strapdown Astro-Inertial Navigation Systems Using Unscented Particle Filtering,"Journal of Computers and Mathematics with Applications, Vol.57, 2009, pp 169-183.

[10] J. Wendel, O. Meister and C. Schlaile, "an Integrated GPS/MEMS-IMU Navigation System for an Autonomous Helicopter,"Journal of Aerospace Science and Technology, Vol.10, 2006, pp.527-533.